A new Southern Ocean species in the remarkable and rare amphipod family Podosiridae (Crustacea: Amphipoda) questions existing systematic hypotheses

OLIVER S. ASHFORD[1,2*,©], TAMMY HORTON[3], CHRISTOPHER N. ROTERMAN[1], MICHAEL H. THURSTON[3], HUW J. GRIFFITHS[4] and ANGELIKA BRANDT[5,6]

[1]*Department of Zoology, University of Oxford, Oxford OX1 3PS, UK*
[2]*Scripps Institution of Oceanography, University of California San Diego, La Jolla, CA 92037, USA*
[3]*National Oceanography Centre, European Way, Southampton SO14 3ZH, UK*
[4]*British Antarctic Survey, High Cross, Madingley Road, Cambridge CB3 0ET, UK*
[5]*Senckenberg Research Institute and Natural History Museum, Department of Marine Zoology, Senckenberganlage 25, 60325 Frankfurt and Main, Germany*
[6]*Goethe University Frankfurt, FB 15 Biological Sciences, Institute for Ecology, Diversity and Evolution, Campus Riedberg, Max-von-Laue-Straße 13, 60438 Frankfurt am Main, Germany*

The amphipod family Podosiridae is unusual in that it combines morphological elements of the disparate families Podoceridae and Eusiridae. Here, we describe a new species in the family from specimens collected from the Southern Ocean in the vicinity of the South Orkney Islands and South Shetland Islands. We present mitochondrial (*COI* and 16S) and nuclear (18S) nucleic acid sequences for this and a congeneric species and use these to investigate the phylogenetic placement of Podosiridae within the Amphipoda. Our results do not provide evidence for a close relationship between Podosiridae and Podoceridae or Eusiridae, suggesting that the superficial similarity between these families is the result of morphological convergence. Instead, it is likely that Podosiridae are more closely related to families within Amphilochidira, such as Stenothoidae. Definitive placement of Podosiridae in the Amphipoda awaits further specimen collection, additional nucleotide data (including sequences from the Hyperiopsidae and the Vitjazianidae) and a more directed analysis of relationships within this portion of the amphipod phylogeny.

ADDITIONAL KEYWORDS: *Acutocoxae ogilvieae* – molecular phylogeny – South Orkney Islands.

INTRODUCTION

The family Podosiridae Lowry & Myers, 2012 is infrequently sampled and is represented by two described species: *Podosirus vaderi* Bellan-Santini, 2007, collected in 2002 from a hydrothermal vent community at 1680 m water depth in the Azores Triple Junction zone (Bellan-Santini, 2007), and *Acutocoxae weddellensis* Rauschert, 2017, collected at 694 m water depth in the Weddell Sea, south of Vestkapp (Rauschert, 2017). Owing to their grasping pereopods,

large gnathopods and elongate maxillipeds, both species are thought to be ambush predators.

The family Podosiridae is notable for its combination of morphological characters from the disparate amphipod families Podoceridae Leach, 1814 and Eusiridae Stebbing, 1888 (Bellan-Santini, 2007). Lowry & Myers (2012) listed significant characters that exclude *Podosirus* from the Eusiridae, Calliopiidae G.O. Sars, 1893 and Pontogeneiidae Stebbing, 1906. Instead, they considered the genus to be most closely related to members of the family Amathillopsidae Pirlot, 1934, based on similarities in body shape, head shape, mouthpart characteristics, the form of gnathopods and pereopods and the shape of pleonites, urosomites and uropods. More recently, a cladistic analysis conducted by Lowry

*Corresponding author. E-mail: oashford@ucsd.edu

& Myers (2017) placed the Podosiridae in its own parvorder, Podosiridira Lowry & Myers, 2017, within the infraorder Hyperiopsida, with the families Hyperiopsidae Bovallius, 1886 and Vitjazianidae Birstein & M. Vinogradov, 1955 as closest relatives.

Between February and March 2016, four specimens resembling the Podosiridae were collected in the vicinity of the South Orkney Islands during the British Antarctic Survey research cruise JR15005 'SO-AntEco' (https://www.bas.ac.uk/project/so-anteco/; last accessed 8 November 19).

Here, we detail the morphology of these Southern Ocean specimens and describe them as a new species. We also present mitochondrial (*COI* and 16S) and nuclear (18S) nucleic acid sequences for these specimens and use this information to investigate the phylogenetic placement of the Podosiridae within the Amphipoda.

MATERIAL AND METHODS

COLLECTION METHODS AND LOCATIONS

The primary material for this study was collected during the British Antarctic Survey expedition 'SO-AntEco' (https://www.bas.ac.uk/project/so-anteco/; last accessed 8 November 19) between February and March 2016 on board the RRS *James Clark Ross* (cruise JR15005) (Griffiths *et al.*, 2016). Podosirids were sampled at three stations at bathyal depths on the South Orkney shelf and slope (775–1139 m; Fig. 1; Table 1). Specimens were taken with a 2-m-wide Agassiz trawl (AGT), with a mesh size of 1 cm.

Collected specimens were fixed in 96% ethanol within minutes of arrival on deck (Griffiths *et al.*, 2016).

An additional specimen collected off Clarence Island (South Shetland Islands) in 1937 (Fig. 1; Table 1) has been found in the Discovery Collections held at the National Oceanography Centre, Southampton (http://noc.ac.uk/facilities/discovery-collections; last accessed 8 November 19).

TAXONOMIC METHODS

Initial observations, dissections and pencil illustrations were made using an Olympus SZX10 stereoscopic microscope with an Olympus SZX-DA camera lucida attachment, and an Olympus BX51 compound microscope with a U-DA camera lucida attachment. Pencil drawings were scanned and inked digitally using Adobe Illustrator and a WACOM digitizer tablet (Coleman, 2003, 2009). Type material is deposited in the Natural History Museum, London, UK (NHMUK).

The adult female holotype specimen (NHMUK 2019. 996) was photographed (Fig. 2) using a Nikon E4500 digital camera mounted to an Olympus SZX10 stereomicroscope with the following settings: F-stop = f/3.2, exposure time = 0.25 s, ISO = 156, exposure bias = –1 step and metering mode = spot.

Setal and mouthpart classifications follow Watling (1989) and Lowry & Stoddart (1992, 1993, 1995). Measurements of inner and outer plates of maxilla 2 and the relative lengths and proportions of pereopods and gnathopods follow Horton & Thurston (2014). Use of the terms 'acute' and 'transverse' relative to the palm of gnathopod 2 follows Poore & Lowry (1997),
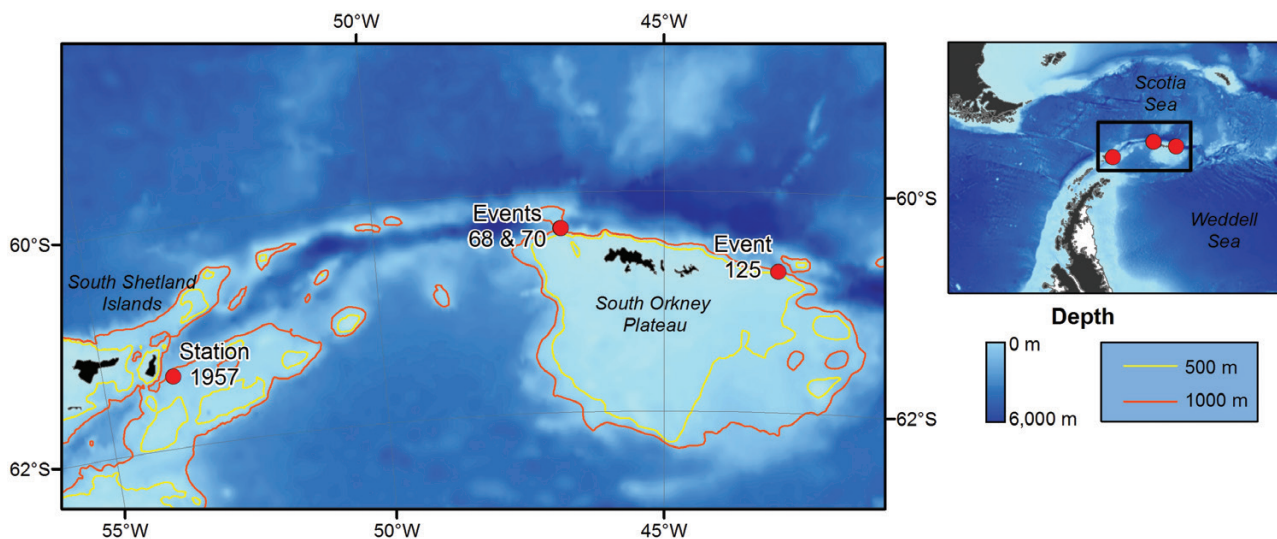
Figure 1. Specimen sampling locations (red dots) and bathymetric context (darker = greater water depth). The 500 m (yellow) and 1000 m (orange) depth contours are displayed. The inset map places specimen sampling locations in a broader context.

Table 1. Details of specimen sampling locations

Cruise	Sample identity	Location	Date	Depth	Gear	Details
SO-AntEco (RRS *James Clark Ross* JR15005)	Event 68, vial 3263	60.3244°S, 46.7701°W	10 March 2016	775 m	Agassiz trawl, 1 cm mesh, 2 m mouth width	Adult male, 25.0 mm. Paratype
SO-AntEco (RRS *James Clark Ross* JR15005)	Event 70, vial 1499	60.3241°S, 46.7694°W	10 March 2016	775 m	Agassiz trawl, 1 cm mesh, 2 m mouth width	Adult female, 25.9 mm. Paratype
SO-AntEco (RRS *James Clark Ross* JR15005)	Event 125, vial 2680.1	60.7206°S, 43.0075°W	16 March 2016	1139 m	Agassiz trawl, 1 cm mesh, 2 m mouth width	Adult female, 24.0 mm. Paratype
SO-AntEco (RRS *James Clark Ross* JR15005)	Event 125, vial 2680.2	60.7206°S, 43.0075°W	16 March 2016	1139 m	Agassiz trawl, 1 cm mesh, 2 m mouth width	Adult female, 25.3 mm. Holotype
RRS *Discovery II* fourth commission	Station no. 1957	61.35°S, 53.75°W	3 February 1937	785–810 m	Large dredge, heavy pattern, 4 ft long	Juvenile female, 11.5 mm. Paratype
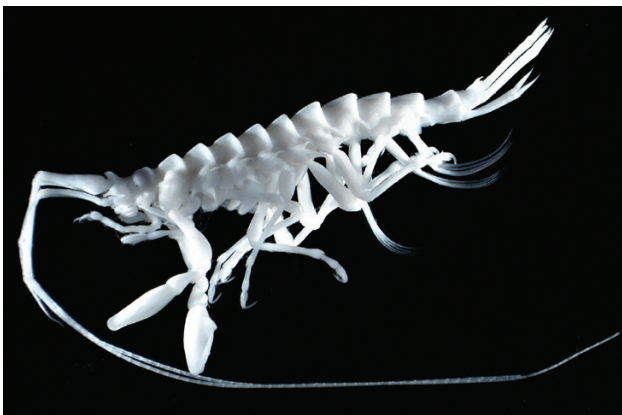
Figure 2. Photograph of *Acutocoxae ogilvieae* holotype; adult female, 25.3 mm, lateral view.

where 'acute' describes the condition in which the included angle between the longitudinal axis of the propodus and the palm is < 90° and 'transverse' the condition in which this angle is ~90°. The species examined here exhibits modification of the propodus of pereopods 3–7. The term 'prehensile' is used where the propodus is expanded to a greater or lesser degree, forming a palm against which the dactylus can close. The palm thus formed is lined with setae noticeably stouter than those on the corresponding margin of the carpus.

The following abbreviations are used: A, antenna; E, epimeron; Ep, epistome; G, gnathopod; LL, lower lip; Md, mandible; Mx, maxilla; Mxp, maxilliped; P, pereopod; T, telson; U, uropod; UL, upper lip; L, left; R, right.

GENETIC METHODS

DNA was extracted from paratype specimens NMHUK 2019. 997 'Event 68, Vial 3263' (adult male, 25 mm) and NMHUK 2019. 998 'Event 70, Vial 1499' (adult female, 25.9 mm) (Table 1). All three left pleopods and pereopod 6 (excluding coxa) were dissected on ice using a sterile scalpel and forceps. Extractions were undertaken using a Qiagen DNeasy Blood and Tissue Kit following the standard 'Purification of Total DNA from Animal Tissues (Spin-Column Protocol)' (2 × 200 μL elutions). DNA concentrations after extraction were estimated using an Invitrogen Qubit 4 fluorometer: 'Event 68, Vial 3263' = 7.60 ng/μL; and 'Event 70, Vial 1499' = 9.54 ng/μL. DNA was also extracted, using the same methodology, from two specimens of *A. weddellensis* ('PS67' and 'PS81') kindly provided by Dr Claude De Broyer, Royal Belgian Institute of Natural Sciences.

Two ribosomal gene regions, 16S (~330 bp) and 18S (~2150 bp) and one protein-coding gene, cytochrome *c* oxidase subunit I (*COI*; ~650 bp) were amplified by polymerase chain reaction (PCR) and sequenced using one or more sets of primers (Table 2). Reactions were performed in 30 μL volumes, containing 2 μL of each primer (forward and reverse at 4 pmol/μL), 15 μL of Qiagen HotStarTaq Plus Master Mix, 5 μL of DNA template and 6 μL of double-distilled water. The PCR cycling protocols for all gene fragments were the same, except for the annealing temperature: an initial denaturation at 95 °C for 5 min, followed by 40 cycles of 94 °C for 45 s, the annealing step for 90 s, 72 °C for 1 min, and a final extension of 5 min at 72 °C. For *COI* and 16S, the annealing temperature was set at 43 °C. For 18S, the annealing step with the primers 18A1 mod

Table 2. List of primers used in this study

Gene	Primer	Sequencing direction	Sequence (5′–3′)	Source
16S	16S_amph_dg_new_F	Forward	GCKGCGGTATWTTGACTGTGCT	This study
16S	16S_amph_dg_new_R	Reverse	RCRTAGAAATTTTAATTCAACATCGAG	This study
COI	crustLCO1491_mod	Forward	TCTACTAACCAYAAAGATATTGG	This study
COI	dg_HCO2198_mod	Reverse	TAAACTTCWGGGTGACCAAAAAATCA	This study
18S	18A1 mod	Forward	CTGGTTGATCCTGCCAGTCATATGC	Raupach *et al.* (2009)
18S	18S_514F	Forward	GCAGCAGGCACGCAAATTACC	This study
18S	A700F mod	Forward	GCCGCGGTAATTCCAGC	Raupach *et al.* (2009)
18S	18S_1275F	Forward	ACCGCCCTAGTTCTAACCYT	This study
18S	18S_1476F	Forward	ACACGGGCMATCTCACCAGG	This study
18S	1800 mod	Reverse	GATCCTTCCGCAGGTTCACCTACG	Raupach *et al.* (2009)
18S	18S_1796R	Reverse	TGCTCTCAGTCTCTKACGRCT	This study
18S	18S_1221R	Reverse	TCGATCCTCTAACTTTCGTTCA	This study
18S	18S_1539R	Reverse	CGCTCCACCAACTAAGAACGGCC	This study
18S	18S_672R	Reverse	CAGCAACTTTAGTAGATG	This study

and 1800 mod (Raupach *et al.*, 2009) was at 56 °C, with additional primers for sequencing. Individuals PS67 and PS81 each generated two smaller 18S fragments (~1200 and ~880 bp long) rather than the single ~2150 bp fragment. The PCRs were performed on a Bio-Rad C1000 Thermal Cycler. PCR clean-up, sequencing reactions and clean-up, in addition to final Sanger sequencing, were undertaken by the Zoology Department sequencing facility at the University of Oxford. Forward and reverse sequences were assembled and cleaned using GENEIOUS v.6.1.8. All sequences are deposited in GenBank (see Supporting Information, Appendix S1 for accession numbers).

GENE ALIGNMENT AND PHYLOGENETIC ANALYSIS

Podosirid *COI*, 18S and 16S gene sequences were added to the GenBank-derived malacostracan sequence alignments produced by Ashford *et al.* (2018) using the 'add' feature of MAFFT v.7.427 (Katoh & Standley, 2013), running on the MAFFT online server (https://mafft. cbrc.jp/alignment/server/; last accessed 8 November 19; G-INS-I alignment strategy). trimAl v1.2 (Capella-Gutiérrez *et al.*, 2009) was used to identify highly variable regions in these genes, which were unlikely to have been aligned reliably. This resulted in the shortening of alignments from 7565 to 1510 bp for 18S, from 811 to 751 bp for 16S, and from 1546 to 444 bp for *COI*. Such an approach has been demonstrated to improve the ratio of phylogenetic signal to noise in alignments (Talavera & Castresana, 2007). Genes were concatenated, along with the *H3* sequence alignment produced by Ashford *et al.* (2018; which was also scrutinized using trimAl v1.2) using SequenceMatrix v.1.8 (Vaidya *et al.*, 2011). Missing sequence data for taxa was coded as '?', and

taxa for which missing data constituted > 50% of the length of their concatenated alignment were removed. After gap removal, this resulted in a final alignment of 2599 bp and 240 concatenated sequences (Supporting Information, Appendix S1).

The optimal model of evolution and partitioning scheme for the concatenated alignment was determined using PartitionFinder v.2.1.1 (Lanfear *et al.*, 2012, 2016), running on the CIPRES Science Gateway v.3.3 online server (Miller *et al.*, 2010). The following settings were specified in the configuration file: branch lengths, unlinked; models of evolution, all; model selection, Bayesian information criterion [BIC; arguably the most appropriate metric of model performance (Abdo *et al.*, 2005; Minin *et al.*, 2003)]; scheme, greedy; data blocks: 16S = 1–318; 18S = 319–1864; *COI* first codon position = 1865–2272\3; *COI* second codon position = 1866–2272\3; *COI* third codon position = 1867–2272\3; *H3* first codon position = 2273–2599\3; *H3* second codon position = 2274–2599\3; and *H3* third codon position = 2275–2599\3. The optimal model of evolution and partitioning scheme for subsequent phylogenetic analyses was found to be the general time reversible model (Tavaré, 1986) plus invariable site proportion plus gamma-distributed rate variation among sites (GTR+I+G) applied across two partitions: 16S, *COI* and *H3* (A) and 18S (B) (BIC score = 157 976.49).

Phylogenies were estimated using both maximum likelihood [ML; RAxML v.8.2.12 (Stamatakis, 2014) and IQ-TREE v.1.6.10 (Nguyen *et al.*, 2014)] and Bayesian (MrBayes v.3.2.6; Ronquist *et al.*, 2012) methodology using the CIPRES Science Gateway v.3.3 online server (Miller *et al.*, 2010). For the ML analyses, RAxML-HPC v.8 on XSEDE and
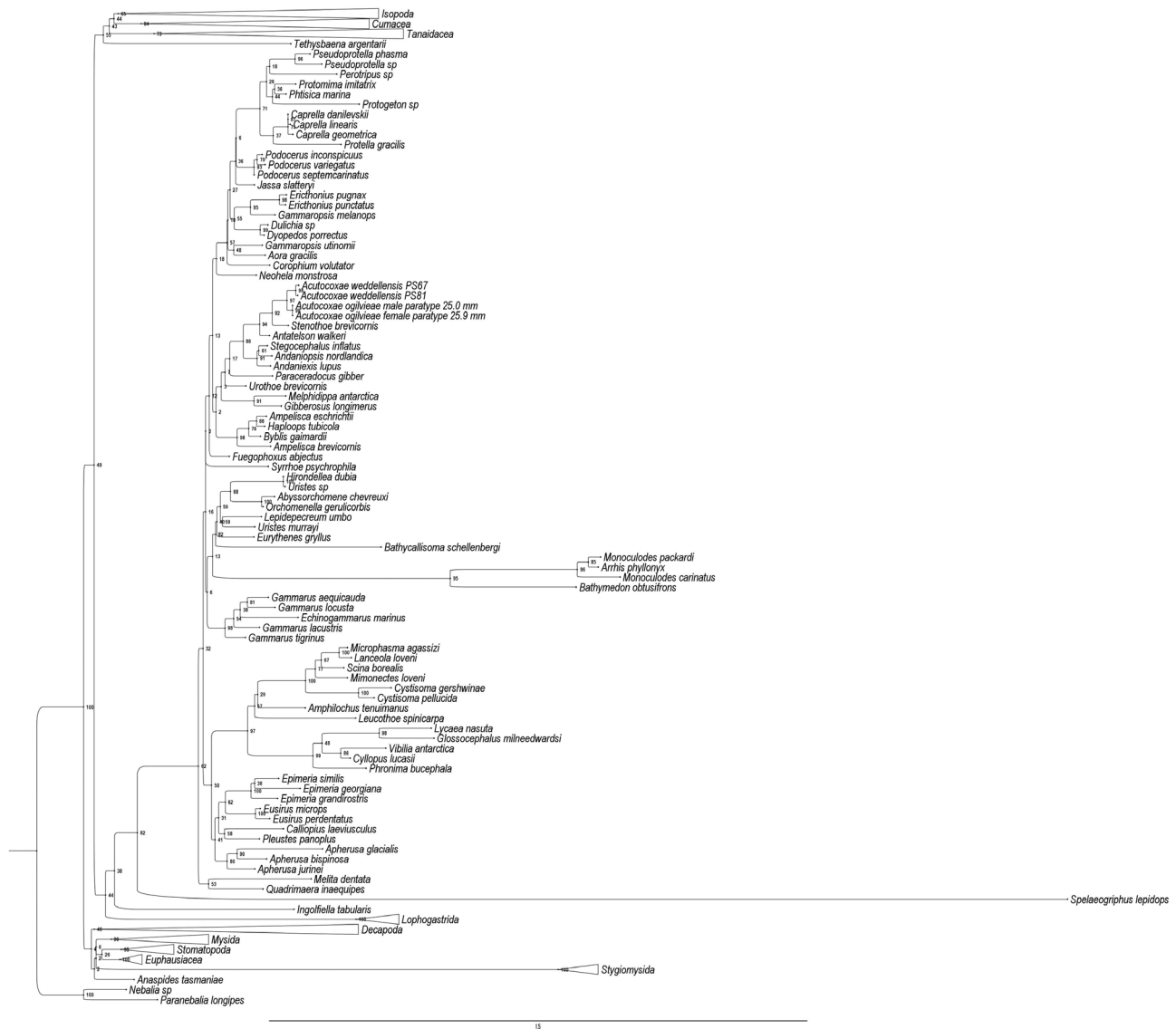
Figure 3. Rooted maximum likelihood phylogeny, placing *Acutocoxae ogilvieae* in the phylogenetic context of 240 malacostracan taxa, estimated using RAxML v.8.2.12. Concatenated dataset of 18S SSU rDNA, 16S rDNA, cytochrome *c* oxidase I (*COI*) and histone *H3* sequence data (2599 bp) analysed under the GTR+I+G model applied across two partitions:16S, *COI* and *H3* (A) and 18S (B). Non-amphipod groups are collapsed. Bootstrap support values (456 rapid bootstraps, halted under autoMRE criterion) are illustrated at branch nodes. The program FigTree v.1.4.4 was used to display the phylogeny. See the Supporting Information (Fig. S1) for the uncollapsed tree.

IQ-TREE on XSEDE were selected. *Nebalia* sp. and *Paranebalia longipes* (Willemöes-Suhm, 1875) (the most basal members of the alignment) were selected as outgroup taxa. The optimal model of evolution and partitioning scheme were specified in accordance with the PartitionFinder results [edge-unlinked partition model with 'more thorough estimation of +I+G model parameters' specified for IQ-TREE (Chernomor *et al.*, 2016)], and a constraint tree forcing order-level taxa to be monophyletic was used. Rapid bootstrapping was specified for the RAxML

analysis, and bootstrapping was halted automatically after 456 bootstraps based on the autoMRE criterion (Fig. 3). Ultrafast bootstrapping (Hoang *et al.*, 2017; 30 000 bootstraps) was specified for the IQ-TREE analysis (Fig. 4). All other parameters were left as default.

For the Bayesian analysis, MrBayes on XSEDE (v.3.2.6) was selected, and all options were specified using a MrBayes data block. *Nebalia* sp. was selected as the outgroup taxon, and trees were constrained to retain order-level monophyly. The optimal model
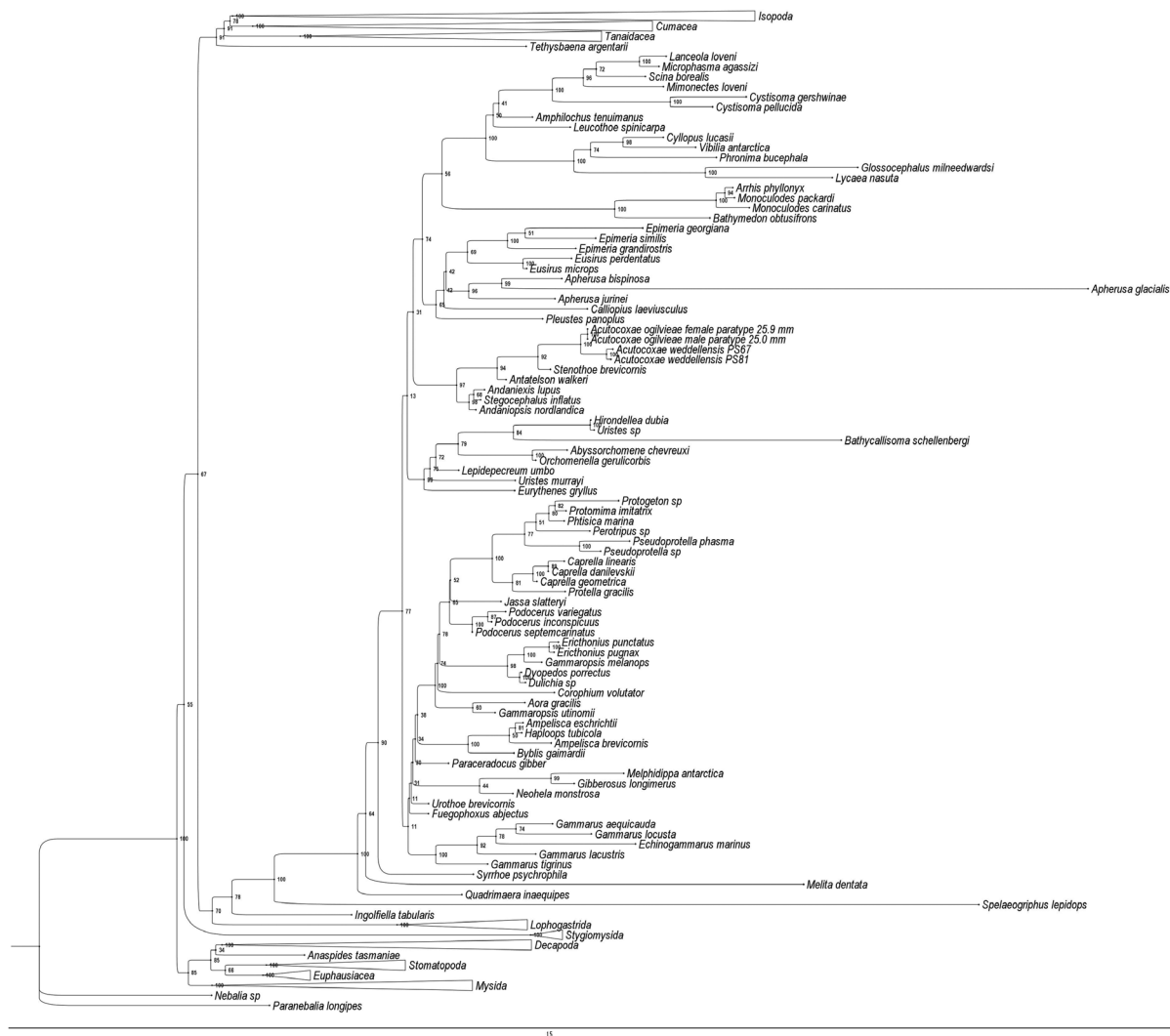
Figure 4. Rooted maximum likelihood phylogeny, placing *Acutocoxae ogilvieae* in the phylogenetic context of 240 malacostracan taxa, estimated using IQ-TREE v.1.6.10. Concatenated dataset of 18S SSU rDNA, 16S rDNA, cytochrome *c* oxidase I (*COI*) and histone *H3* sequence data (2599 bp) analysed under the GTR+I+G model applied across two partitions: 16S, *COI* and *H3* (A) and 18S (B). Non-amphipod groups are collapsed. Bootstrap support values (30 000 ultrafast bootstraps) are illustrated at branch nodes. The program FigTree v.1.4.4 was used to display the phylogeny. See the Supporting Information (Fig. S2) for the uncollapsed tree.

of evolution and partitioning scheme were defined in accordance with the PartitionFinder results, with parameters unlinked and rates free to vary such that each partition could evolve under independent scenarios. Two runs were specified, with trees sampled every 2000 generations, using eight Markov chains with a heating value of 0.12. The two runs converged (standard deviation of split frequencies < 0.01) after 20 530 000 generations. A burn-in of 10% was selected, corresponding to stabilization of sample probabilities as determined using TRACER v.1.6 (Rambaut *et al.*, 2013), and a 50% majority rule consensus tree was constructed from the remaining trees (Fig. 5).

RESULTS

SYSTEMATICS

ORDER AMPHIPODA LATREILLE, 1816

SUBORDER HYPERIOPSIDEA BOVALLIUS, 1886

INFRAORDER HYPERIOPSIDA BOVALLIUS, 1886

PARVORDER PODOSIRIDIRA LOWRY & MYERS, 2012

SUPERFAMILY PODOSIRIOIDEA LOWRY & MYERS, 2012
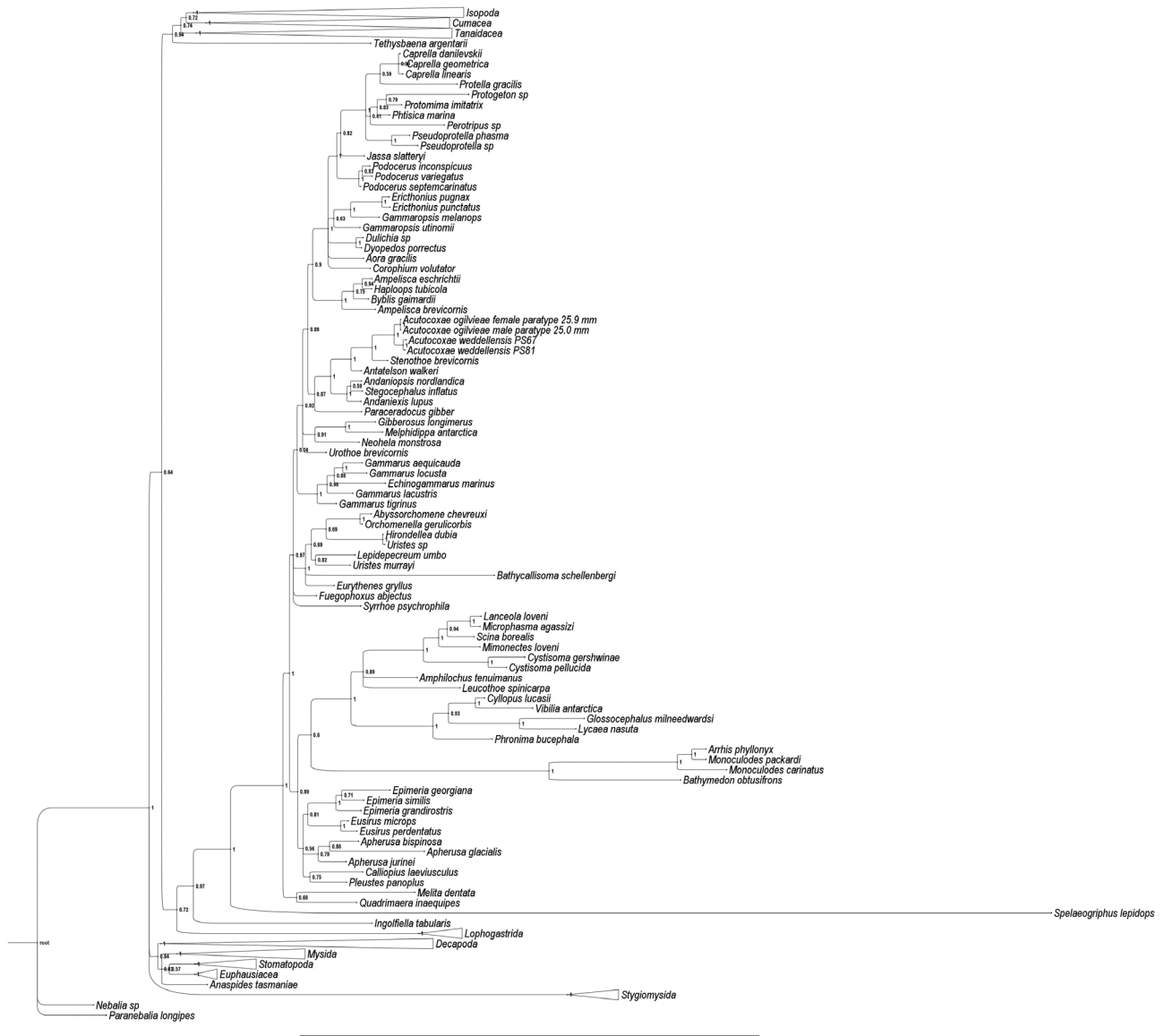
Figure 5. Rooted Bayesian phylogeny (50% majority rule consensus), placing *Acutocoxae ogilvieae* in the phylogenetic context of 240 malacostracan taxa, estimated using MrBayes v.3.2.6. Concatenated dataset of 18S SSU rDNA, 16S rDNA, cytochrome *c* oxidase I (*COI*) and histone *H3* sequence data (2599 bp) analysed under the GTR+I+G model applied across two partitions: 16S, *COI* and *H3* (A) and 18S (B). Non-amphipod groups are collapsed. Posterior probabilities are illustrated at branch nodes. The program FigTree v.1.4.4 was used to display the phylogeny. See the Supporting Information (Fig. S3) for the uncollapsed tree.

FAMILY PODOSIRIDAE LOWRY & MYERS, 2012
(AMENDED)

Debroyeridae Rauschert, 2017: 11 (nomen nudum)

Diagnostic description

Pereon *dorsoventrally flattened*; without setae. Head *as long as* or longer than deep; eyes *present or* absent. Antenna 1 peduncle *with few* or no setae;

accessory flagellum absent; primary flagellum 5 or more articulate; callynophore absent; calceoli *absent*. Antenna 2 with sparse slender setae; flagellum longer *or shorter* than peduncle; flagellum 5 or more articulate. Mouthparts well developed, forming a subquadrate bundle. Mandible incisor dentate, straight; *lacinia mobilis* broad, apically dentate; molar present, medium sized, strongly triturating *or forming an apically toothed conical flap*; palp 3-articulate *or reduced to*

1-articulate. Maxilla 1 inner plate apically setose (setae vestigial *or reduced to a single large seta*); palp *medium to* large, 2-articulate *or reduced to 1-articulate*. Maxilla 2 inner plate shorter than outer plate, without oblique setal row. Maxilliped, *inner and outer plates small, vestigial or absent*; palp enlarged, raptorial.

Pereon: Pereonites smooth and rounded *or carinate with strong lateral extensions*. Pereonite 7 with small dorsal carina *or not*. Coxae 1–7 well developed. Coxae 1–4 short, broader than long, *weakly* overlapping *or not*. Coxa 4 without posterodistal lobe. Coxa 5 *with* or without lobes. Gnathopod 1 smaller than gnathopod 2; dissimilar in form to gnathopod 2; subchelate; coxa smaller than coxa 2; anteroventral corner produced, acute. Gnathopod 2 subchelate; coxa subequal in size to *or smaller than coxa 3*; dactylus well developed. Pereopods 3–7 basis linear; merus linear, much longer than propodus; carpus linear. Pereopods 3–4 not glandular. Pereopod 4 coxa subequal in size to coxa 3, without posteroventral lobe. Pereopods 5–7 *subequal in length and similar in structure*.

Pleon: Pleonites carinate. Urosome *laterally compressed*; urosomites 1–3 free. Urosomite 1 *longer or* much longer than urosomite 2. Uropods 1–2 similar in size and structure; apices of rami without robust setae. Uropod 1 peduncle without basofacial robust seta, without ventromedial spine. Uropod 3 biramous *or uniramous*. Telson laminar, longer than broad, *suboval*, entire.

Remarks

Bellan-Santini (2007) discussed the similarities of the new genus *Podosirus* in relation to the families Eusiridae *s.l.* and Podoceridae. Lowry & Myers (2012) listed significant characters that exclude *Podosirus* from the Eusiridae, Calliopiidae and Pontogeneiidae and considered it to be most closely related to the Amathillopsidae. Rauschert (2017) raised a new family, Debroyeridae, for his new genus and species *A. weddellensis*. According to the International Commission on Zoological Nomenclature (ICZN, 1999) Articles 11.7.1.1, 16.2 and 29.1, a new family name must be derived from the name of the type genus, and therefore Debroyeridae is invalid and should be considered a *nomen nudum*. The Rauschert paper is a private publication and is undated. However, a copy sent to one of the authors (M.H.T.) was accompanied by a covering letter dated '08.05.2017'.

Acutocoxae shows precisely the same characters of agreement and disagreement with Eusiridae *s.l.*, Podoceridae and Amathillopsidae as does *Podosirus*, hence our decision to place the genus in the Podosiridae.

We are unsure whether *Acutocoxae* fits within this family, but for the sake of stability we have included it here until further data are available. In order to place the new species in the family Podosiridae, we have made significant amendations to the family diagnosis provided by Lowry & Myers (2012) (italicized statements in the *Diagnostic description* section above). A re-measurement of pereopods 5–7, based on Bellan-Santini's habitus illustrations of *P. vaderi*, suggests that these appendages are in fact subequal, contrary to the family diagnosis provided by Lowry & Myers (2012) (the relative lengths of pereopods 5–7, including coxae, in *P. vaderi* are 1:1.00:0.97; in *Acutocoxae ogilvieae* 1:0.97:0.94). Lowry & Myers (2012) indicate that coxae 4–5 are without lobes, but *P. vaderi* does possess a posterior lobe on pereopod 5. The two species show similarities in the gnathopods and pereopods, but this could be a result of convergent evolution. The structure of the head in the two genera differs markedly. The body of *Acutocoxae* is armed with lateral extensions of the pereonites, coxae and the head lobes, which are not present in *Podosirus*. The coxae of *Acutocoxae* are discontiguous, but there is some degree of overlap in *Podosirus*. The mouthparts of *Podosirus* and our new species show some similarities, but the mandibular palp in *Acutocoxae* is reduced to a single article, and the maxilliped has lost the outer lobes completely, has the inner lobes reduced and fused, and the palp is developed into an enormous raptorial organ. Our interpretation of the habitus illustration of Bellan-Santini (2007) differs from that of Lowry & Myers (2012) in that we believe that the pereon is dorsoventrally flattened rather than subcylindrical and the urosome is likely to be laterally compressed or subcylindrical. This can be confirmed only by examination of the type material, which we have not seen.

GENUS *ACUTOCOXAE* RAUSCHERT, 2017 (AMENDED)

Type species: Acutocoxae weddellensis Rauschert, 2017.

Diagnosis

Body slender, dorsoventrally flattened, carinate dorsally and laterally. Rostrum moderate; lateral cephalic lobe strongly produced, acute. Eyes present. Antenna 1 much longer than body, peduncle article 1 much longer than the head, article 2 longer than article 1, article 3 short, accessory flagellum absent. Antenna 2 slender. Labrum weakly bilobed. Mandibular molar a toothed flap, incisor process multidentate, *lacinia mobilis* on left mandible only (in *A. ogilvieae*), as broad as incisor; palp uniarticulate. Maxilla 1 inner plate small with a single robust terminal seta, outer plate with large terminal robust setae. Maxilla 2 inner plate short, shorter than outer. Maxilliped basal article elongate,

reflexed posteriorly; inner plates very small, fused or not; outer plates absent; palp very elongate, strongly raptorial, 4-articulate, dactylus recurved, longer than article 3, minutely serrate.

Coxae 1–2 short, with single acute antero- or ventrolaterally directed processes. Coxae 3–4 short, with two acute antero- and posterolaterally directed processes. Coxae 5–7 short, with single acute posterolaterally directed processes. Gnathopod 2 larger than gnathopod 1, subchelate. Pereopods 3–7 strongly prehensile, basis linear, not lobate. Epimeral plate 3 subquadrate. Urosomite 1 longer than 2 and 3 combined, without dorsal teeth. Uropods 1–3 peduncles much longer than rami. Uropod 3 uniramous. Telson entire, suboval, without setae.

Remarks

Specimens of the new species exhibit the slender, dorsoventrally flattened body, moderate rostrum, lack of accessory flagellum, extended, raptorial maxilliped, acuminate coxae, elongate urosomite 1 and entire telson that are seen in the genus *Podosirus*. However, the genus *Acutocoxae* differs from *Podosirus* in the strongly produced lateral cephalic lobes, presence of eyes, ratio of antenna 1 articles, elongate peduncles of uropods 1–3 and uniramous uropod 3.

A revised diagnosis of the genus *Acutocoxae* Rauschert, 2017 is provided. Rauschert (2017) indicated that *A. weddellensis* possesses a rudimentary accessory flagellum. Our examination of the type material reveals a group of small setae, but no accessory flagellum. No accessory flagellum was found in our new species. Rauschert (2017) provided an illustration of the mandibular molar, which he described as having a 'strong elevation for grinding'. We have been unable to examine this, because both mandibles are missing from the type material. This is different from the toothed flap molar found in our new species. Eyes are prominent, hemispherical, and similar to those of some species in the family Melphidippidae Stebbing, 1899.

ACUTOCOXAE OGILVIEAE HORTON, ASHFORD & THURSTON **SP. NOV.**

(FIGS 6–12)

LSID: urn:lsid:zoobank.org:act:CE72904F-BC27-4A05-86FF-2B0A2A51E7C8

Type material

Holotype: Female, 25.3 mm, NHMUK 2019. 996; Event 125, Vial 2680.2, 60.7206°S, 43.0075°W, 1139 m depth, 16 March 2016, Agassiz Trawl, 2 m mouth width, 1 cm mesh.

Paratypes: Adult male, 25.0 mm, NMHUK 2019. 997; Event 68, Vial 3263, 60.3244°S, 46.7701°W, 775 m depth, 10 March 2016, Agassiz trawl.

Adult female, 25.9 mm, NMHUK 2019. 998; Event 70, Vial 1499, 60.3241°S, 46.7694°W, 775 m depth, 10 March 2016, Agassiz trawl.

Adult female, 24.0 mm. NMHUK 2019. 999; Event 125, Vial 2680.1, 60.7206°S, 43.0075°W, 1139 m, 16 March 2016, Agassiz trawl.

Juvenile female, 11.5 mm, NHMUK 2019. 1000; Station number 1957, 61.35°S, 53.75°W, off south side of Clarence Island, 7 miles East of Cape Bowles, South Shetlands, 785–810 m depth, 3 February 1937, Large Dredge, Heavy Pattern, 4 ft (1.2 m) long (Table 1).

Type locality

Southern Ocean, 60.7206°S 43.0075°W, 1139 m.

Description

Holotype female, 25.3 mm.

Body: Dorsoventrally flattened, well calcified, keeled from pereonite 2 to urosomite 1; pereonite 2 to pleonite 3 with posterior transverse ridge; pereonite 2–6 with lateral flanges, with posterior extensions; flange strongest on pereonite 2.

Head: Exposed, saddle shaped; eye lobe produced, narrow and acute, projecting laterally at ~45°; rostrum raised, short and rounded. *Eyes:* present, large, hemispherical, white. *Antenna 1:* elongate (incomplete), length ≥ 1.6 × body; peduncle article 1 long, bulbous proximally, length 3 × breadth at broadest point, without posterodistal spine or lobe; article 2 very long, length 1.4 × article 1, slender, with a few small robust setae dorsally and ventrally; article 3 short, length 0.25 × article 1; flagellum long, > 60-articulate, callynophore absent, calceoli absent, accessory flagellum absent. *Antenna 2:* articles 4 and 5 elongate, article 5 0.9 × article 4, both with sparse slender robust setae dorsally; flagellum well developed, incomplete, calceoli absent.

Mouthpart bundle: Subquadrate. *Epistome:* bulbous. *Upper lip:* weakly bilobed. *Mandible:* incisors dentate, symmetrical, weak, cutting edge convex, with ten or 11 teeth; *lacinia mobilis* on left mandible only, broad, apically with ten teeth; left spine row with four large, robust setae and a dense aggregation of slender setae, right with two prominent acute teeth and slender setae; molar present, medium in size, forming an apically toothed conical flap; palp attached level with molar, 1-articulate, left palp with six slender setae,
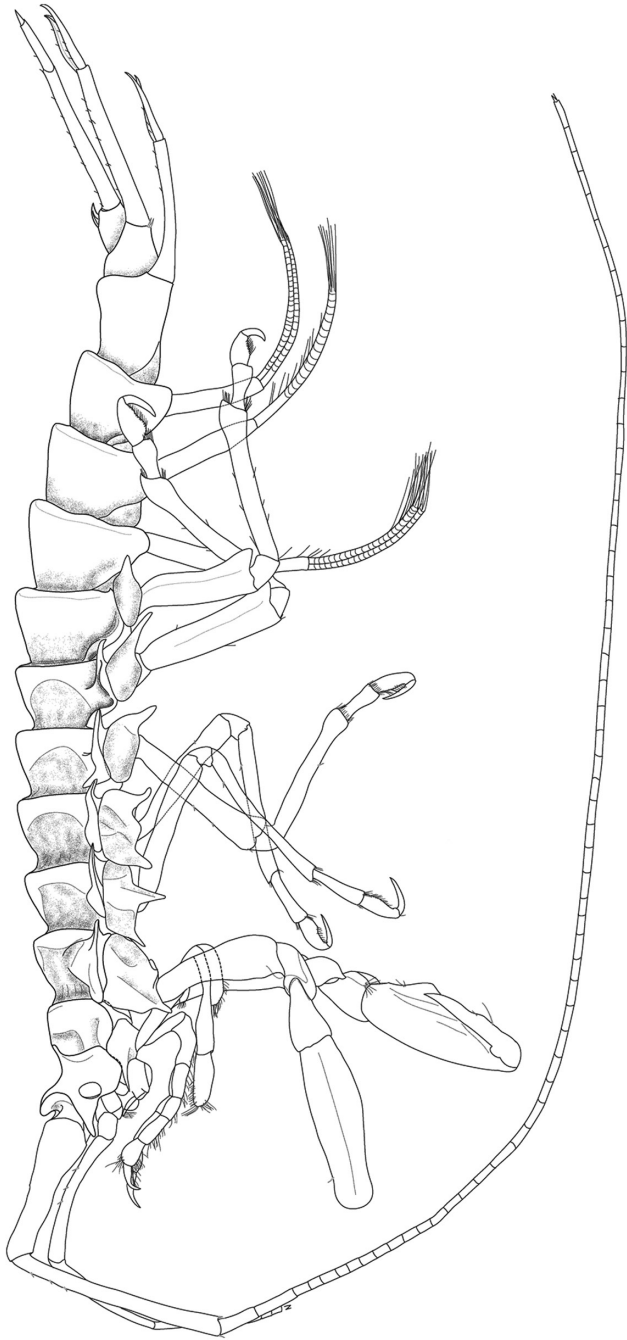
Figure 6. *Acutocoxae ogilvieae* holotype; adult female, 25.3 mm, habitus, lateral view.
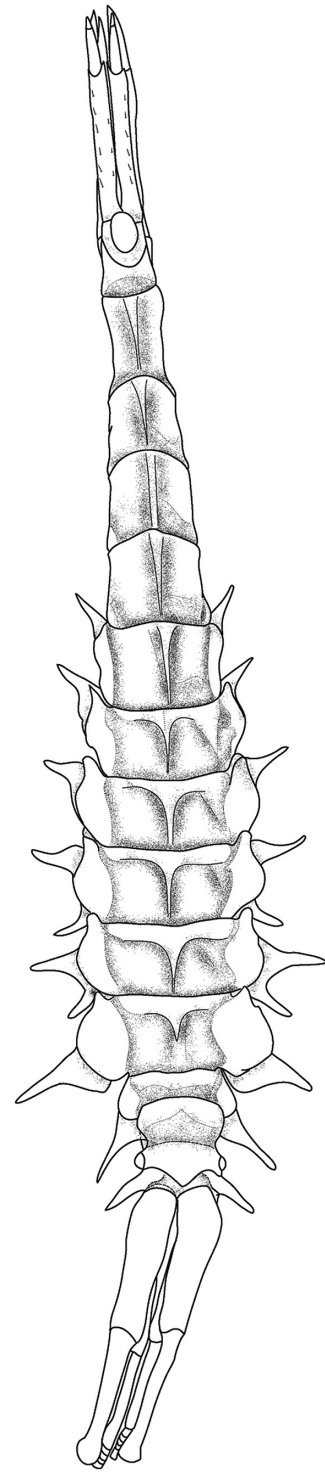
Figure 7. *Acutocoxae ogilvieae* holotype; adult female, 25.3 mm, habitus, dorsal view.

right palp with ten slender setae. *Maxilla 1:* inner plate small, with a single large robust seta apically; outer plate with six large slender robust setae apically and five much smaller slender robust setae subapically; palp, 1-articulate with nine robust setae on oblique apical margin. *Maxilla 2:* weak, inner plate shorter than outer, setose. *Maxilliped:* basal article elongate, reflexed posteriorly, subequal to article 2; inner plates very small, fused; outer plates absent; palp very elongate, strongly raptorial, 4-articulate, dactylus recurved, longer than article 3, minutely serrate.

Gnathopod 1: Subchelate; coxa short, smaller than coxa 2, strong tooth acutely produced, projecting anterolaterally; basis long, slender, weakly expanded; ischium short; merus with posterodistal lobe; carpus longer than propodus; propodus weakly expanded, dorsal surface with numerous short setae, palm acute with three robust setae at palmar angle, dactylus shorter than palm. *Gnathopod 2:* subchelate; coxa short, strong tooth acutely produced, projecting ventrolaterally; basis long, strongly expanded with acute tooth anterodistally; ischium short, produced anterodistally; carpus subtriangular, posterodistally lobate; propodus large, robust, length 1.8 × breadth, palm acute, with a U-shaped central excavation between a rounded proximal tooth and two rounded distal teeth; dactylus robust, reaching palmar corner. *Pereopod 3:* prehensile; coxa short, strong teeth anteriorly and medially acutely produced, projecting ventrolaterally; basis long, margins parallel; merus slender, subequal to basis; carpus 0.37 × length of merus; propodus weakly expanded medially, 0.74 × carpus, posterior margin with 16 robust setae; dactylus robust, as long as palm. *Pereopod 4:* coxa short, strong teeth anteriorly and posteriorly acutely produced, projecting ventrolaterally; basis long, margins parallel; merus slender, shorter than basis; carpus 0.33 × merus; propodus, weakly expanded medially, 0.87 × carpus, posterior margin with 15 robust setae; dactylus robust, as long as palm. *Pereopod 5:* coxa short, strong tooth posteriorly acutely produced, projecting ventrolaterally; basis long, margins parallel, expanded posterodistally to a large acute flange; merus slender, subequal to basis; carpus 0.27 × length of merus; propodus weakly expanded medially, subequal to carpus, posterior margin with 17 robust setae; dactylus robust, as long as palm. *Pereopod 6:* similar to pereopod 5 except coxa more strongly produced posteriorly; basis flange produced
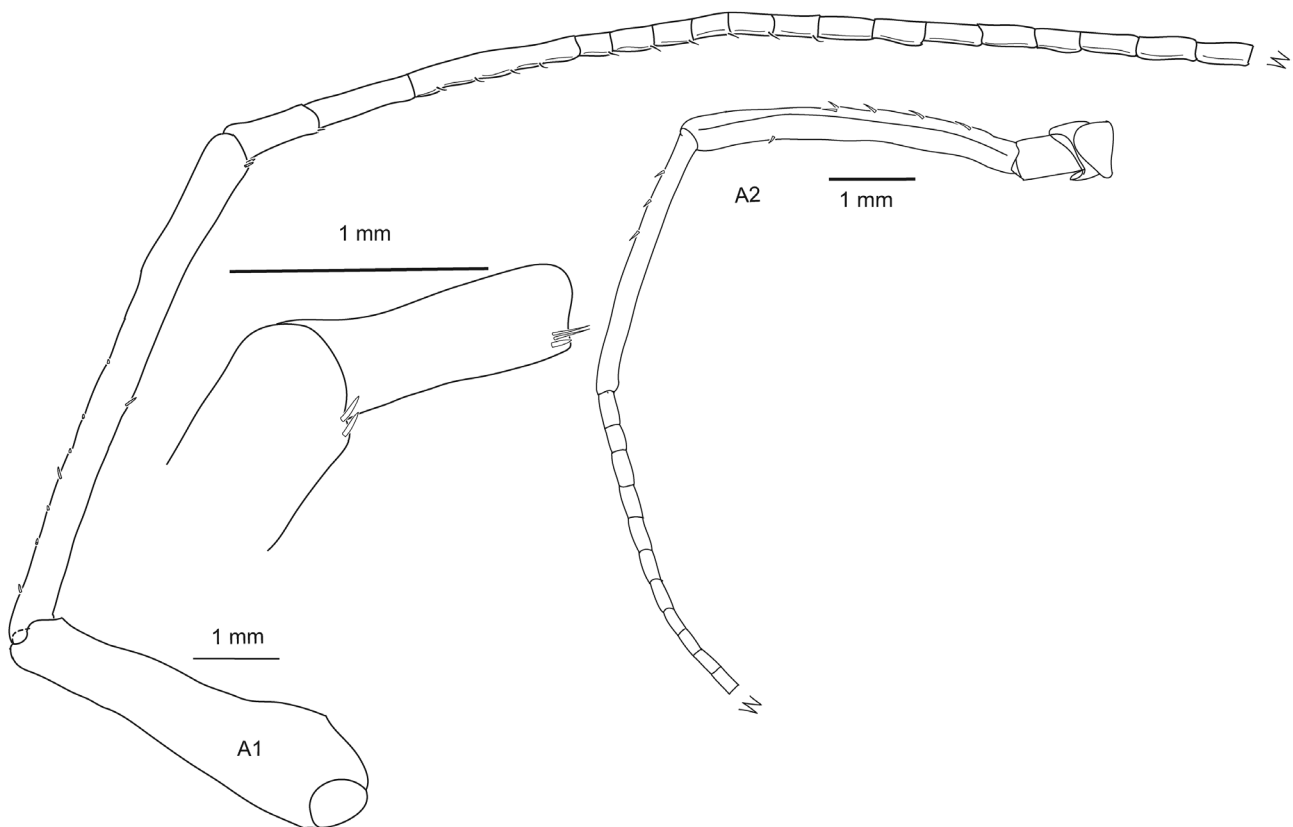
Figure 8. *Acutocoxae ogilvieae* holotype; adult female, 25.3 mm, antennae.
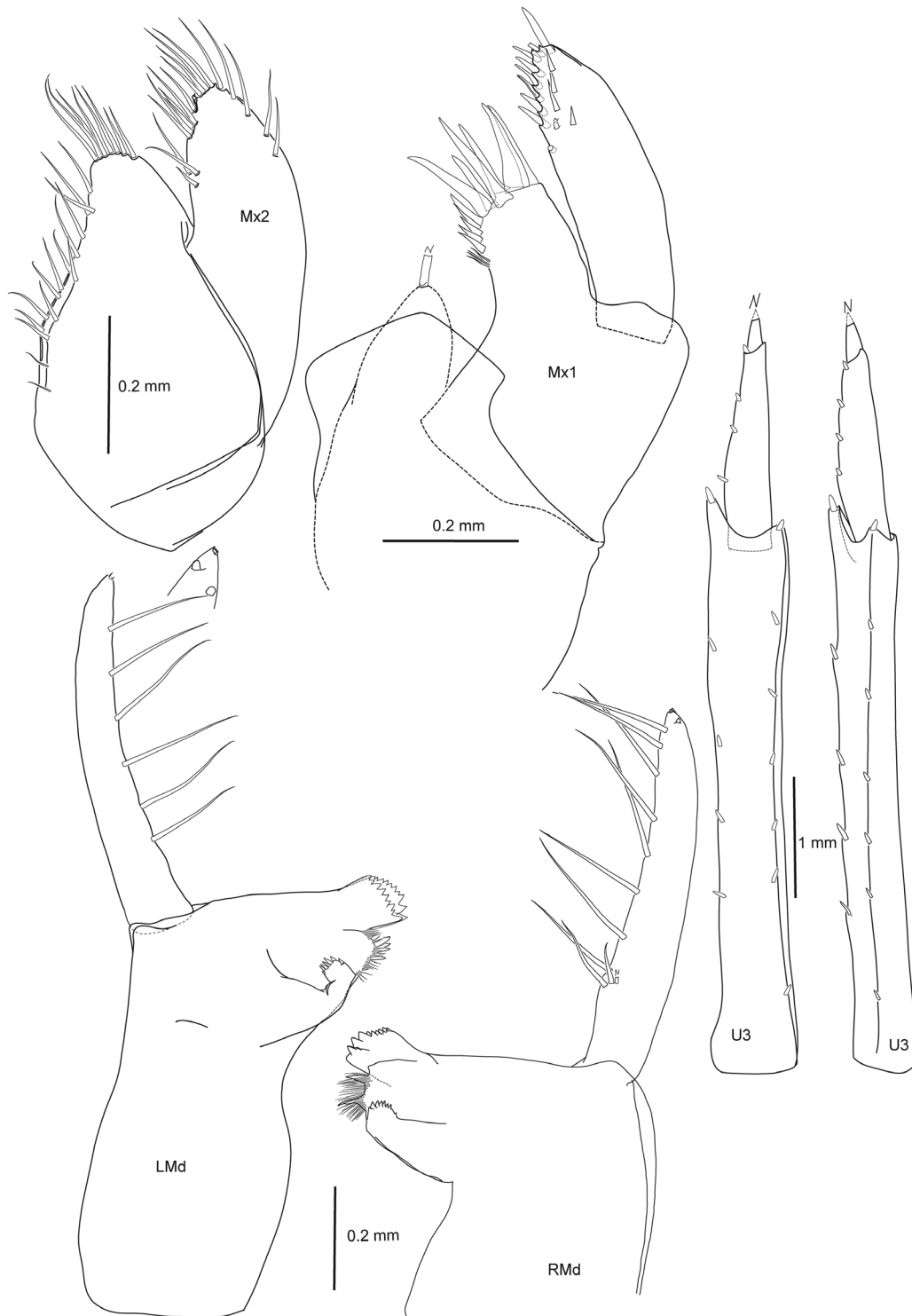
Figure 9. *Acutocoxae ogilvieae*. holotype; adult female, 25.3 mm, maxilla 1, maxilla 2, left and right mandible and uropod 3 (both LHS, dorsal and slightly rotated view).

along greater extent of length; distal expansions of merus and propodus more pronounced; merus 1.2 × basis; propodus 1.2 × carpus, posterior margin with 20 robust setae; dactylus shorter than palm. *Pereopod 7:* similar to pereopod 6 except acute posterior process of coxa ~0.5 × length of equivalent process on pereopod 6;
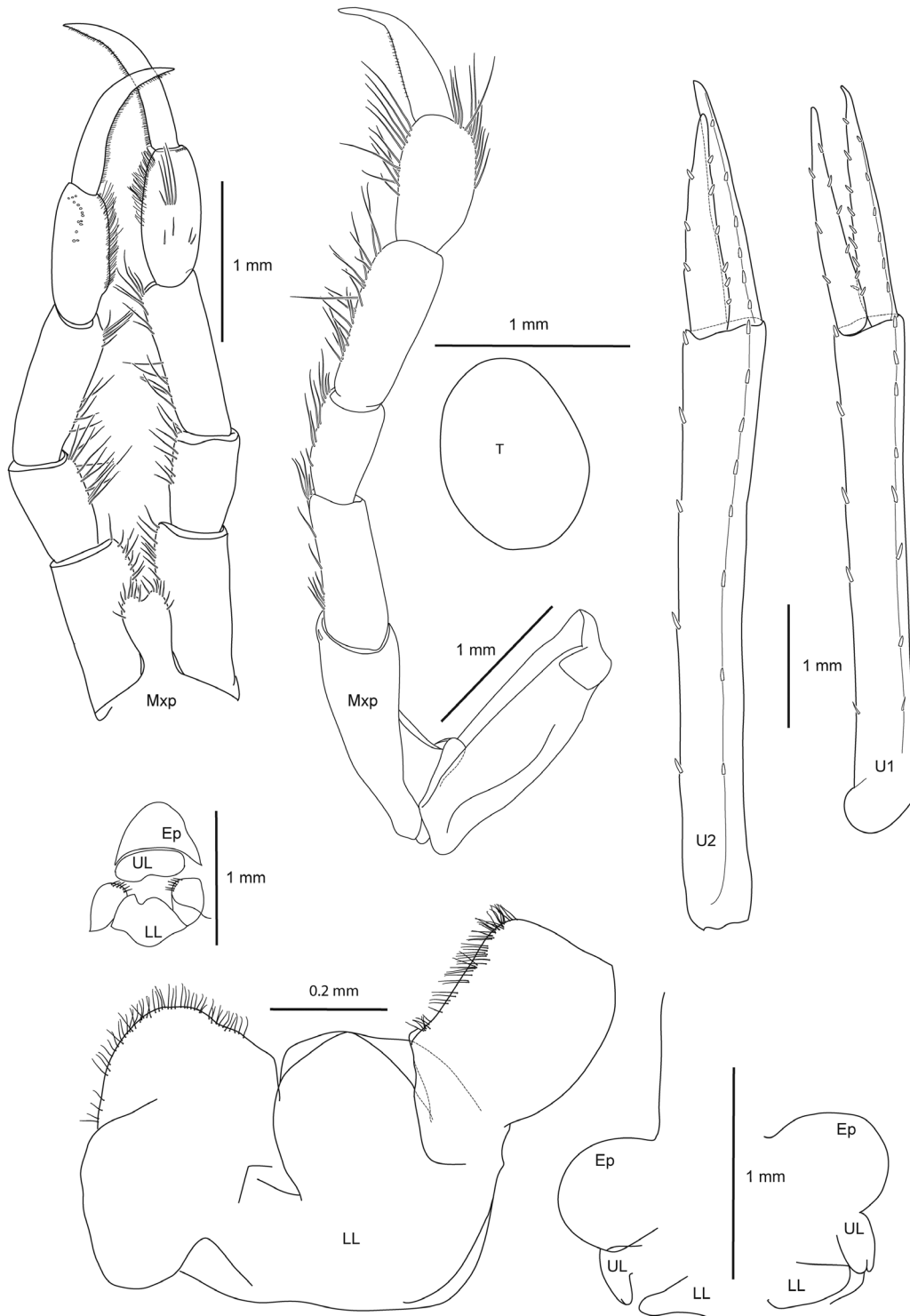
Figure 10. *Acutocoxae ogilvieae* holotype; adult female, 25.3 mm, maxilliped (dorsal and lateral view), epistome, upper lip, lower lip, telson and uropods 1 and 2.

distal expansions of merus and propodus stronger than pereopod 6; merus 1.3 × basis; carpus 0.28 × merus; posterior margin with 24 robust setae.

Gills: Normal, present on gnathopod 2 to pereopod 6. *Oostegites:* present on gnathopod 2 to pereopod 5, suboval. *Epimera:* ridged anteriorly. *Epimeron 1:*
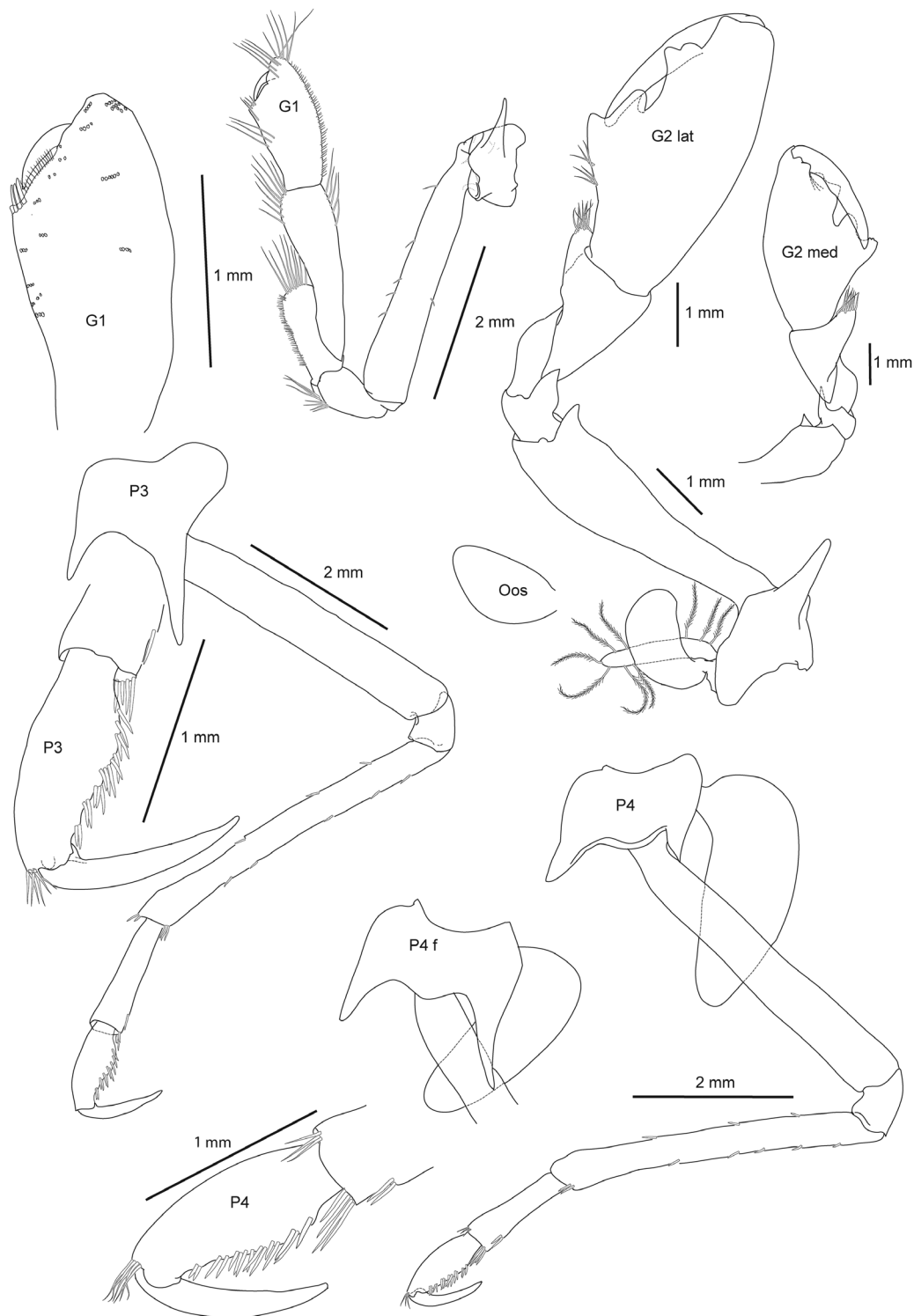
Figure 11. *Acutocoxae ogilvieae* holotype; adult female, 25.3 mm, gnathopod 1, gnathopod 2 (medial and lateral view), pereopods 3 and 4 and oostegite.

rounded posteriorly. *Epimeron 2:* subquadrate posteriorly. *Epimeron 3:* quadrate posteriorly, posterior margin weakly convex. *Urosomites:* free, urosomite 1 longer than combined lengths of urosomites 2 and 3. *Uropod 1:* peduncle long, with five robust setae medially and eight robust setae laterally; rami 0.45 ×
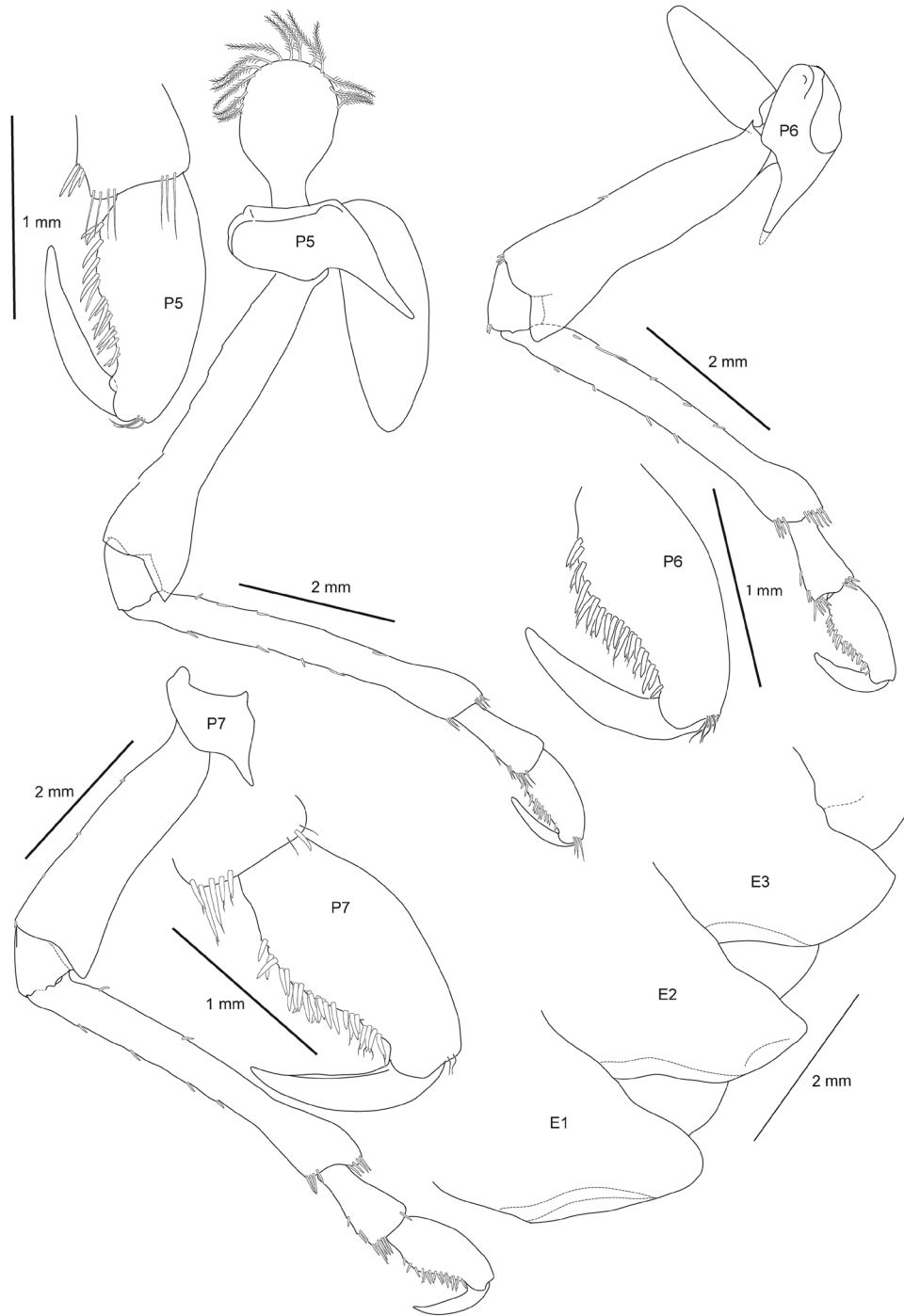
Figure 12. *Acutocoxae ogilvieae* holotype; adult female, 25.3 mm, gnathopod 1, gnathopod 2 (medial and lateral view), pereopods 5–7 and epimera.

peduncle; outer ramus 1.05 × length of inner ramus, with eight robust setae medially and five robust setae laterally; inner ramus with three robust setae medially and six robust setae laterally. *Uropod 2:* peduncle long, 1.2 × uropod 1 peduncle, with five robust setae medially and eight robust setae laterally;

rami 0.39 × peduncle, outer ramus 1.1 × length of inner ramus, with nine robust setae medially and six robust setae laterally; inner ramus with three robust setae medially and six robust setae laterally. *Uropod 3:* peduncle long, subequal to uropod 2, with medial projection and five robust setae medially and seven

robust setae laterally; uniramous, 0.44 × peduncle; ramus biarticulate, article 2 0.20 × article 1; article 1 with four robust setae medially. *Telson:* entire, oval, length 1.3 × breadth, without setae.

Etymology

This species is named as a noun in a genitive case after the maiden name (Ogilvie) of Imogen Catherine Rachel Ashford, wife to author O.S.A.

Sexual dimorphism

None.

Remarks

The new species appears to be similar to the only other species in the genus, *A. weddellensis*. We have studied all available type material of that species and found inconsistencies between the material and the illustrations and description provided by Rauschert (2017). *Acutocoxae weddellensis* is in the process of redescription, using new material (C. De Broyer, personal communication). The two species can be separated easily by the form of the propodus on pereopods 3–7, with the posterior margins of pereopods 3 and 4 and the anterior margins of pereopods 5–7 convex and expanded medially in *A. ogilvieae* and narrow and strongly concave in *A. weddellensis*.

Depth range

775–1139 m.

Distribution

Southern Ocean (South Orkney Islands, South Shetland Islands).

PHYLOGENY

The conducted ML (RAxML and IQ-TREE) and Bayesian (MrBayes) analyses suggest, with high support, that the two species of *Acutocoxae* form a monophyletic group, but appear to be distinct species (Figs 3–5). This is in agreement with the morphological observations and supported by *COI* and 16S raw pairwise distances between the species of 10.7 and 3.2%, respectively (Tempestini *et al.*, 2018).

Of the crustacean taxa included in our phylogenetic analyses, the genus *Acutocoxae* appears to be most closely related to the stenothoid amphipod species *Antatelson walkeri* (Chilton, 1912) and *Stenothoe brevicornis* Sars, 1882. This is inferred, with high support, from both ML and Bayesian analyses (Figs 3–5). In turn, in all phylogenetic trees presented, there is high support for a sister-group relationship between this podosirid/stenothoid clade and species of the amphipod family Stegocephalidae Dana, 1852 (Figs 3–5).

Deeper phylogenetic relationships differ among the three trees presented, and node support values are generally low. However, there is little support for a close relationship between *Acutocoxae* and any of the podocerid or eusirid species analysed (Figs 3–5).

DISCUSSION

Our ability to place *Acutocoxae* in phylogenetic context within the Amphipoda is somewhat restricted by the low support values for moderately deep nodes in the constructed phylogenies, which is reflected by differences in the phylogenetic results provided by the alternative analysis methods (Figs 3–5). Our phylogenies, coupled with the analysis of Bousfield (1983) and the supertree of Peracarida presented by Ashford *et al.* (2018), suggest that difficulties in resolving deeper nodes within the phylogeny of the Amphipoda might stem from rapid diversifications of amphipod lineages, possibly during the early Carboniferous period and later during the Mesozoic. Deeper nodes may be more completely resolved in future phylogenetic studies by incorporating both morphological and molecular data (Wortley & Scotland, 2006). However, even considering the problems in resolving deeper nodes here, there is little support for a close relationship between *Acutocoxae* and any of the eusirid or podocerid taxa included in our analyses, suggesting that the apparent similarity of the Podosiridae to the Podoceridae and Eusiridae (Bellan-Santini, 2007) reflects morphological convergence.

Lowry & Myers (2012) also rejected a close relationship between the Podosiridae and Eusiridae and listed several characters that exclude *Podosirus* from Eusiridae, Calliopiidae and Pontogeneiidae. Our revision of the diagnosis of the Podosiridae does not significantly contradict their arguments. Instead, Lowry & Myers (2012) argued that the Podosiridae are most closely related to the family Amathillopsidae. Core characters shared between podosirids and amathillopsids include elongate raptorial maxillipedal palps, subchelate gnathopods, linear bases to pereopods 5–7, pereopods with elongate meri and a relatively elongate urosomite 1. Diagnostic characters shared between podosirids and amathillopsids include coxa 1 smaller than coxa 2, pereopods 5–7 (sub)equal in length, pleonites dorsally carinate and telson entire. However, podosirids differ significantly from amathillopsids by lacking an accessory flagellum,

by the carpus of gnathopod 1 being longer than the propodus and by gnathopod 1 being smaller than gnathopod 2.

Congruence between ML and Bayesian trees, and high node support values, provide confidence that, of the peracarid taxa included in the phylogenetic analyses conducted here, *Acutocoxae* is most closely related to the amphipod family Stenothoidae Boeck, 1871. However, whilst *Acutocoxae* exhibits characteristics of some stenothoids, such as lack of an accessory flagellum, a reduced mandibular molar and palp, an absence of maxilliped outer plates, an enlarged gnathopod 2, coxa 4 without posterodorsal excavation, uniramous uropod 3 and entire telson, it is unlikely that *Acutocoxae* resides in Stenothoidae, because it lacks key diagnostic characteristics of the family; in particular, a small coxa 1 that is partly covered by the following coxae, and an enlarged, shield-like coxa 4 (Barnard & Karaman, 1991). It is possible that the Podosiridae is closely related to Stenothoidae or that the genus *Acutocoxae* resides in a family that is closely related to Stenothoidae but not included in our analyses. However, to test this hypothesis further would require a more directed and in-depth analysis of relationships within this part of the amphipod phylogeny, which is beyond the scope of the present study.

Based on a cladistic analysis of amphipod morphology, Lowry & Myers (2017) concluded that Podosiridae form a distinct clade in the infraorder Hyperiopsida, with the families Hyperiopsidae and Vitjazianidae as closest relatives. Although we cannot explicitly rule out this hypothesis, owing to incomplete taxon sampling (nucleotide data are not available in GenBank for members of either of these families at present), the seemingly close relationship between *Acutocoxae* and Stenothoidae suggests an alternative affinity for Podosiridae within the parvorder Amphilochidira. This would be in agreement with the conclusion by Lowry & Myers (2012) that Podosiridae might have a relatively close relationship to Amathillopsidae. The diagnoses of Amphilochidira and Hyperiopsida offered by Lowry & Myers (2017) are relatively similar (Table 3). However, the diagnosis of *Acutocoxae* we provide appears to have more similarities with Amphilochidira than it does with Hyperiopsida (Table 3). However, we concede that the definitive placement of Podosiridae within Amphipoda will require further specimen collection, additional nucleotide data (including sequences from Hyperiopsidae and Vitjazianidae) and a more directed analysis of relationships within this portion of the amphipod phylogeny.

Finally, the apparent close relationship between Stenothoidae and Stegocephalidae and the apparent distance of Stegocephalidae from the remaining lysianassidiran taxa in our phylogenies are noteworthy. This counters the current phylogenetic placement of Stegocephalidae within Lysianassidira (Lowry & Myers, 2017).

ACKNOWLEDGEMENTS

Table 3. Comparison of diagnosis of *Acutocoxae* (provided by the present study) with those of Hyperiopsidea and Amphilochidira [provided by Lowry & Myers (2017)]

Morphological region	*Acutocoxae*	Hyperiopsida	Amphilochidira
Body	Dorsoventrally flattened	Laterally compressed	Laterally compressed or dorsoventrally flattened
Mandibular molar	Small, non-triturative	Triturative	Small and non-triturative, or absent
Maxilliped palps	Well developed	Well developed	Well developed
Coxae	Small	Small	Large or small
Pereopod 4 coxa	With two acute antero- and posterolaterally directed processes	Without posteroventral lobe	Variable in form
Uropods 1–2 rami	Without apical robust setae	Without apical robust setae	Without apical robust setae

REFERENCES

Abdo Z, **Minin V**, **Joyce P**, **Sullivan J. 2005.** Accounting for uncertainty in the tree topology has little effect on the decision-theoretic approach to model selection in phylogeny estimation. *Molecular Biology and Evolution* **22:** 691–703.

Ashford OS, **Kenny AJ**, **Barrio Frojan CRS**, **Bonsall MB**, **Horton T**, **Brandt A**, **Bird GJ**, **Gerken S**, **Rogers AD. 2018.** Phylogenetic and functional evidence suggests that deep-ocean ecosystems are highly sensitive to environmental change and direct human disturbance. *Proceedings of the Royal Society B: Biological Sciences* **285:** 20180923.

Barnard JL, **Karaman GS. 1991.** The families and genera of marine gammaridean Amphipoda (except marine gammaroids). Part 2. *Records of the Australian Museum Supplement* **13:** 419–866.

Bellan-Santini D. 2007. New amphipods of hydrothermal vent environments on the Mid-Atlantic Ridge, Azores triple junction zone. *Journal of Natural History* **41:** 567–596.

Bousfield EL. 1983. An updated phyletic classification and palaeohistory of the Amphipoda. In: Schram FR, ed. *Crustacean phylogeny*. Rotterdam: A.A. Balkema, 257–277.

Capella-Gutiérrez S, **Silla-Martínez JM**, **Gabaldón T. 2009.** trimAl: a tool for automated alignment trimming in large-scale phylogenetic analyses. *Bioinformatics* **25:** 1972–1973.

Chernomor O, **von Haeseler A**, **Minh BQ. 2016.** Terrace aware data structure for phylogenomic inference from supermatrices. *Systematic Biology* **65:** 997–1008.

Coleman CO. 2003. "Digital inking": how to make perfect line drawings on computers. *Organisms Diversity & Evolution* **3:** 303–304.

Coleman CO. 2009. Drawing setae the digital way. *Zoosystematics and Evolution* **85:** 305–310.

Griffiths HJ, **Allcock AL**, **Ashford OS**, **Blagbrough HJ**, **Brandt A**, **Brasier MJ**, **Danis B**, **Downey RV**, **Eleaume MP**, **Enderlein P**, **Grant SM**, **Ghiglione C**, **Hogg OT**, **Lens PCD**, **Mackenzie MK**, **Macfee C**, **Moreau CVE**, **Preston M**, **Robinson LF**, **Rodriguez E**, **Spiridonov V**, **Tate AJ**, **Taylor MI**, **Waller CL**, **Wiklund H. 2016.** RRS James Clark Ross *JR15005 cruise report, South Orkneys – state of the Antarctic ecosystem*. Cambridge, UK: British Antarctic Survey, 149.

Hoang DT, **Chernomor O**, **von Haeseler A**, **Minh BQ**, **Vinh LS. 2017.** UFBoot2: improving the ultrafast bootstrap approximation. *Molecular Biology and Evolution* **35:** 518–522.

Horton T, **Thurston MH. 2014.** A revision of the bathyal and abyssal necrophage genus *Cyclocaris* Stebbing, 1888 (Crustacea: Amphipoda: Cyclocaridae) with the addition of two new species from the Atlantic Ocean. *Zootaxa* **3796:** 507–527.

ICZN. **1999.** *International code of zoological nomenclature*. London: International Trust for Zoological Nomenclature.

Katoh K, **Standley DM. 2013.** MAFFT multiple sequence alignment software version 7: improvements in performance and usability. *Molecular Biology and Evolution* **30:** 772–780.

Lanfear R, **Calcott B**, **Ho SYW**, **Guindon S. 2012.** PartitionFinder: combined selection of partitioning schemes and substitution models for phylogenetic analyses. *Molecular Biology and Evolution* **29:** 1695–1701.

Lanfear R, **Frandsen PB**, **Wright AM**, **Senfeld T**, **Calcott B. 2016.** PartitionFinder 2: new methods for selecting partitioned models of evolution for molecular and morphological phylogenetic analyses. *Molecular Biology and Evolution* **34:** 772–773.

Lowry JK, **Myers AA. 2012.** Podosiridae, a new family of North Atlantic deep sea amphipod. *Zootaxa* **3546:** 81–84.

Lowry JK, **Myers AA. 2017.** A phylogeny and classification of the Amphipoda with the establishment of the new order Ingolfiellida (Crustacea: Peracarida). *Zootaxa* **4265:** 1–89.

Lowry JK, **Stoddart HE. 1992.** A revision of the genus *Ichnopus* (Crustacea: Amphipoda: Lysianassoidea: Uristidae). *Records of the Australian Museum* **44:** 185–245.

Lowry JK, **Stoddart HE. 1993.** Crustacea Amphipoda: lysianassoids from Philippine and Indonesian waters. In: Crosnier A, ed. *Résultats des campagnes MUSORSTOM*. Paris: ORSTOM, 55–109.

Lowry JK, **Stoddart HE. 1995.** New lysianassoid genera and species from south-eastern Australia (Crustacea: Amphipoda). *Records of the Australian Museum* **47:** 7–25.

Miller MA, **Pfeiffer W**, **Schwartz T. 2010.** Creating the CIPRES Science Gateway for inference of large phylogenetic trees. In: *Gateway Computing Environments Workshop (GCE), 2010*. New Orleans: IEEE, 1–8.

Minin V, **Abdo Z**, **Joyce P**, **Sullivan J. 2003.** Performance-based selection of likelihood models for phylogeny estimation. *Systematic Biology* **52:** 674–683.

Nguyen L-T, **Schmidt HA**, **von Haeseler A**, **Minh BQ. 2014.** IQ-TREE: a fast and effective stochastic algorithm for estimating maximum-likelihood phylogenies. *Molecular Biology and Evolution* **32:** 268–274.

Poore AGB, **Lowry JK. 1997.** New ampithoid amphipods from Port Jackson, New South Wales, Australia (Crustacea: Amphipoda: Ampithoidae). *Invertebrate Taxonomy* **11:** 897–941.

Rambaut A, **Suchard MA**, **Xie W**, **Drummond AJ. 2013.** *Tracer: MCMC trace analysis tool*, *1.6th edn*. Edinburgh.

Raupach MJ, **Mayer C**, **Malyutina M**, **Wägele J-W. 2009.** Multiple origins of deep-sea Asellota (Crustacea: Isopoda) from shallow waters revealed by molecular data. *Proceedings of the Royal Society B: Biological Sciences* **276:** 799–808.

Rauschert M. 2017. *Neue Gammariden aus dem Weddellmeer*. Berlin: published by the author. Available at: http://tree.bio.ed.ac.uk/software/tracer/ (accessed 8 May 2017).

Ronquist F, **Teslenko M**, **Van der Mark P**, **Ayres DL**, **Darling A**, **Höhna S**, **Larget B**, **Liu L**, **Suchard MA**, **Huelsenbeck JP. 2012.** MrBayes 3.2: efficient Bayesian phylogenetic inference and model choice across a large model space. *Systematic Biology* **61:** 539–542.

Stamatakis A. 2014. RAxML version 8: a tool for phylogenetic analysis and post-analysis of large phylogenies. *Bioinformatics* **30:** 1312–1313.

Talavera G, **Castresana J. 2007.** Improvement of phylogenies after removing divergent and ambiguously aligned blocks from protein sequence alignments. *Systematic Biology* **56:** 564–577.

Tavaré S. 1986. Some probabilistic and statistical problems in the analysis of DNA sequences. *Lectures on Mathematics in the Life Sciences* **17:** 57–86.

Tempestini A, **Rysgaard S**, **Dufresne F. 2018.** Species identification and connectivity of marine amphipods in Canada's three oceans. *PLoS ONE* **13:** e0197174.

Vaidya G, **Lohman DJ**, **Meier R. 2011.** SequenceMatrix: concatenation software for the fast assembly of multi-gene datasets with character set and codon information. *Cladistics* **27:** 171–180.

Watling L. 1989. A classification system for crustacean setae based on the homology concept. In: Felgenhauer BE, Watling L, Thistle AB, eds. *Functional morphology of feeding and grooming in Crustacea*. Boca Raton: CRC Press, 15–27.

Wortley AH, **Scotland RW. 2006.** The effect of combining molecular and morphological data in published phylogenetic analyses. *Systematic Biology* **55:** 677–685.

SUPPORTING INFORMATION

Additional Supporting Information may be found in the online version of this article at the publisher's web-site:

Appendix S1. Taxonomic identity and GenBank accession number for all genetic sequences analysed.

Figure S1. Rooted maximum likelihood phylogeny, placing *Acutocoxae ogilvieae* in the phylogenetic context of 240 malacostracan taxa, estimated using RAxML v.8.2.12. Concatenated dataset of 18S SSU rDNA, 16S rDNA, cytochrome *c* oxidase I (*COI*) and histone *H3* sequence data (2599 bp) analysed under the GTR+I+G model applied across two partitions: 16S, *COI* and *H3* (A) and 18S (B). Bootstrap support values (456 rapid bootstraps, halted under autoMRE criterion) are illustrated at branch nodes. FigTree v.1.4.4 was used to display the figure. Please contact author O.S.A. for a Newick-format copy of the phylogeny.

Figure S2. Rooted maximum likelihood phylogeny, placing *Acutocoxae ogilvieae* in the phylogenetic context of 240 malacostracan taxa, estimated using IQ-TREE v.1.6.10. Concatenated dataset of 18S SSU rDNA, 16S rDNA, cytochrome *c* oxidase I (*COI*) and histone *H3* sequence data (2599 bp) analysed under the GTR+I+G model applied across two partitions: 16S, *COI* and *H3* (A) and 18S (B). Bootstrap support values (30 000 ultrafast bootstraps) are illustrated at branch nodes. FigTree v.1.4.4 was used to display the figure. Please contact author O.S.A. for a Newick-format copy of the phylogeny.

Figure S3. Rooted Bayesian phylogeny (50% majority rule consensus), placing *Acutocoxae ogilvieae* in the phylogenetic context of 240 malacostracan taxa, estimated using MrBayes v.3.2.6. Concatenated dataset of 18S SSU rDNA, 16S rDNA, cytochrome *c* oxidase I (*COI*) and histone *H3* sequence data (2599 bp) analysed under the GTR+I+G model applied across two partitions: 16S, *COI* and *H3* (A) and 18S (B). Posterior probabilities are illustrated at branch nodes. FigTree v.1.4.4 was used to display the figure. Please contact author O.S.A. for a Newick-format copy of the phylogeny.